



P-340

## Basin Configuration of the Kutch Rift Basin from High Resolution Aeromagnetic Data

*Mita Rajaram\* and S.P. Anand, Indian Institute of Geomagnetism*

### Summary

High resolution aeromagnetic (HRAM) data collected recently over the Kutch Rift Basin have been analysed to look below the salt plains, grassland and sediments and to understand the Basin configuration of this seismically active region. The analysis has been able to identify several hitherto unknown dykes, sedimentary basins, faults and intrusive and throws light on the depositional history of the Deccan traps. The Banni Plains depict a ridge and depression structure and we identify aureole like structures within the Banni Plains which could possibly be related to hydrocarbon formations. We find that the epicenter of the Bhuj earthquake lies on the intersection of three subsurface faults and the faults are related to the directional change of the compressional forces on either side of the Bhuj epicenter, as calculated by GPS measurements. The epicenter of the aftershocks are constrained to lie within an area demarcated by these three faults. Through the modeling of aeromagnetic data along a seismic reflection section passing through Bhuj and Anjar, we estimate the depth of the fault. The study brings out the importance of aeromagnetic data in study of regions with large surface cover and the important role of integrated geophysical studies.

**Keywords:** High resolution aeromagnetic data, Kutch Rift Basin, Hydrocarbon, seismotectonics

### Introduction

The Kutch rift basin of Gujrat (Zone V) has witnessed occurrence of high intensity earthquakes; the catastrophic Bhuj earthquake of 26 January 2001 with magnitude Mw 7.8 being the most damaging in the last 50 years. Several Geophysical studies have been undertaken to understand this intra-plate earthquake in a region covered by Runn of Kutch (salt flats), Banni plains (grassland) and sediments; however, several enigmatic questions remain unanswered. Recently, high resolution aeromagnetic (HRAM) total magnetic field data were collected by Directorate General of Hydrocarbons over the Kutch Rift Basin. The objective of the survey was to acquire high resolution magnetic data to map the anomalous magnetic field distribution pattern in order to understand the lithology and sub surface structural settings in aid of geological interpretation. Here we analyze this recently acquired HRAM data over the Kutch Rift Basin to look below the surface cover and understand the Basin configuration and identify tell tale signatures associated with the earthquake.

### Results and Discussions

The paper explores the utility of HRAM data to look below the surface cover and bring out the Basin configuration. Techniques like differential reduction to pole (as the area under study is in a relatively low geomagnetic latitude) (Arkani Hamed, 2007), second vertical derivative to decipher shallow structures (Blakely, 1995) and located Euler depths (Blakely and Simpson, 1986) are used in addition to the spectral depth estimates, the 3D Euler deconvolution method (Reid et al, 1990) and forward modeling of the data.

By using a combination of the above mentioned methods, the analysis is able to bring out signatures of several hitherto unknown sedimentary basins, dykes, faults and intrusives. Most of the high frequency anomalies are related to exposed and subsurface theolitic trap flows while circular to elliptical anomalies represent alkaline intrusive into the Precambrian basement that might have resulted during the pre-rift period or syn-rift phase of the basin formation. Traps have been identified to the north of the Kutch Mainland fault for the first time thus having implications on the depositional history of the traps. Several



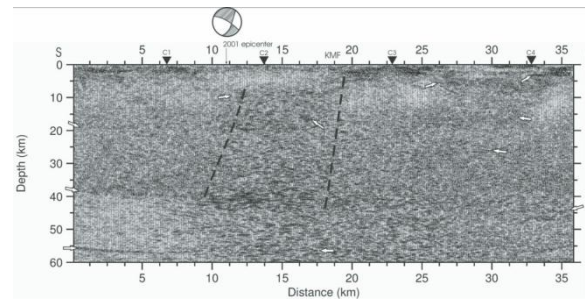
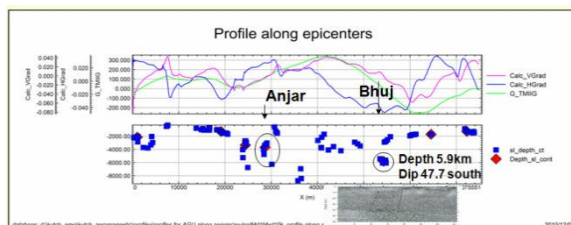
## Basin Configuration of the Kutch Rift Basin from HRAM Data



dykes are identified east of Lodai suggesting that this region has undergone extensional tectonics. The boundary of the Banni basin is delineated bounded by NNE-SSW trending faults in the east and west and EW faults in the north and south. Seismotectonic analysis has been undertaken using a combination of the aftershock data, GPS strain vectors and the newly identified faults from the aeromagnetic data. Through such an analysis we were able to infer that the epicenter of the main shock of Bhuj earthquake sits on the intersection of three subsurface faults. The epicenters of aftershocks are constrained to lie within an area defined by the newly identified faults. The NW-SE and NE-SW faults emanating from the main epicenter form a V shaped pattern that are related to the directional change of the compressional forces on either side of the Bhuj epicenter, as seen in the GPS data. Reactivation of these subsurface faults may be the causative factor for the Bhuj earthquake.

Crustal structure and nature of this seismogenic region was generated along few profiles through the modeling of aeromagnetic data using available information from other geophysical and geological studies as constraints.

Integrating magnetic data with the seismic reflection data along a profile through Bhuj and Anjar (shown below), it was found that one among the three intersecting faults (~EW fault) discussed above, is at an average depth of 6km and dipping south and continuing up to Moho level. From Euler solutions it can be seen that this fault runs in a WNW-ESW direction. Few aftershocks in the depth range from 2-10km are reported in this area (Reena de et.al, 2003). The fault responsible for Anjar earthquake is also evident on the Euler solution, at a depth of almost 4km.



Pre-stack depth migrated section along a profile running across the 2001 epicentral region. Prominent reflection boundaries are represented by white arrows. Hypocenter of the Bhuj earthquake along with the focal mechanism as viewed on a vertical cross section is also shown. Moho is at a depth of 38-45km. (Sarkar et al, 2007).

Detailed analysis of the western sub-basin of the Banni basin has been carried out and depth estimates are calculated using spectral method. RTP map shows that the western sub-basin is characterized by a NW-SE elliptical magnetic high at an average depth of 2.5km from the surface representing basaltic intrusive into the Precambrian basement. From spectral estimates the average sediment thickness of this region is approximately 3km. This suggests that the basaltic body have intruded into the sediments. Basaltic flows are identified to the west of basin boundary fault, in the SVD map. An annular/aureole-shaped sub nT anomaly overlying the alluvial covered region is observed on the northern side of the western sub-basin. High resolution aeromagnetic data interpretation by Stone et al (2004) have identified aureole type magnetic anomalies over oil fields and they interpreted that these usually sub nT amplitude anomalies are associated with near-surface magnetite deposits generated predominantly from microbial alteration of hematite to magnetite in the presence of hydrocarbon micro-seepage. Hence we infer that the sub nT anomaly can possibly be a micro magnetic anomaly associated with hydrocarbon seepage which require further detailed studies. An annular/aureole shaped anomaly observed within the basin can possibly be related to the building-up of magnetite via intra and extra cellular processes associated with hydrocarbon micro seepage. Depth estimates suggest that the western basin is itself having a ridge and depression structure composed of thick



## Basin Configuration of the Kutch Rift Basin from HRAM Data



sediments in the central part. Two wells, Banni 2 and Nirona, were drilled by ONGC. The depth to the basement at Banni2 calculated by spectral estimates is around 1.83km which is comparable with the drilled depth of 1.7645 to the granitic basement. A comparison of the basement depth (in meters) calculated using power spectral method, located Euler and the wells drilled in two regions of the banni basin along with the inferred basement lithology is given in the table (it may be noted that the depth estimates using located Euler solutions could vary up to  $\pm 15\%$ ).

Well	Lithology of Basement	Well depth (m)	power spectrum depth (m)	Located Euler Depth
Banni2	Granitic basement	1764.5	1830	2100 $\pm$ 315
Nirona	Trachytic basement	2224.45	2510	2000 $\pm$ 300

### Conclusions

The analysis of the HRAM over the seismically active Kutch Rift Basin could identify several hitherto unknown faults, dykes, intrusive etc that throw light on the Basin configuration and tectonics of this rifted sedimentary basin. Detailed studies on the western sub-basin of the Banni basin have identified annular sub nT anomalies that probably represent hydrocarbon seepage related to the building up of magnetite through intra and extra cellular processes. From integrated analysis of magnetic, GPS, seismological and seismic reflection studies we find that the Bhuj epicenter sits on the junction of three faults trending NW-SE, NE-SW and WNW-ESE and the aftershocks are constrained to lie within an area defined by these faults. The NW-SE & NE-SW faults emanating from main epicenter are perpendicular to the directional change of the compressional forces on either side of the Bhuj epicenter, as calculated by GPS measurements. The basin configuration and other detailed results of these studies will be presented.

### References

- Arkani-Hamed, J., 2007. Differential Reduction to the Pole – Revisited. *Geophysics* 72, L13-L20.
- Blakely, R.J., 1995. *Potential theory in Gravity and Magnetic applications*. Cambridge University Press, Australia.
- Blakely, R.J., Simpson, R.W., 1986. Approximating edges of source bodies from magnetic or gravity anomalies. *Geophysics* 51, 1494-1498.
- Reid, A.B., Allsop, J.M., Granser, H Miliett, A.J., Somerton, W.I., 1990. Magnetic interpretations in three dimensions using Euler deconvolution. *Geophysics* 55, 80-91.
- Reena De et.al, 2003. *Proc. Indian Acad. Sci. (E&P.)*, 112, No. 3, p. 413-419
- Sarkar et al, 2007. *GSA, Special paper* 425, p.319-327.
- Stone, V.C.A., Fairhead, J.D., Oterdoom, W.H., 2004. *Micromagnetic seep detection in the Sudan. The Leading Edge*, 734-737.